Supplementary Information

Tumor-reprogrammed resident T cell resist radiation to control tumors

Arina et al.

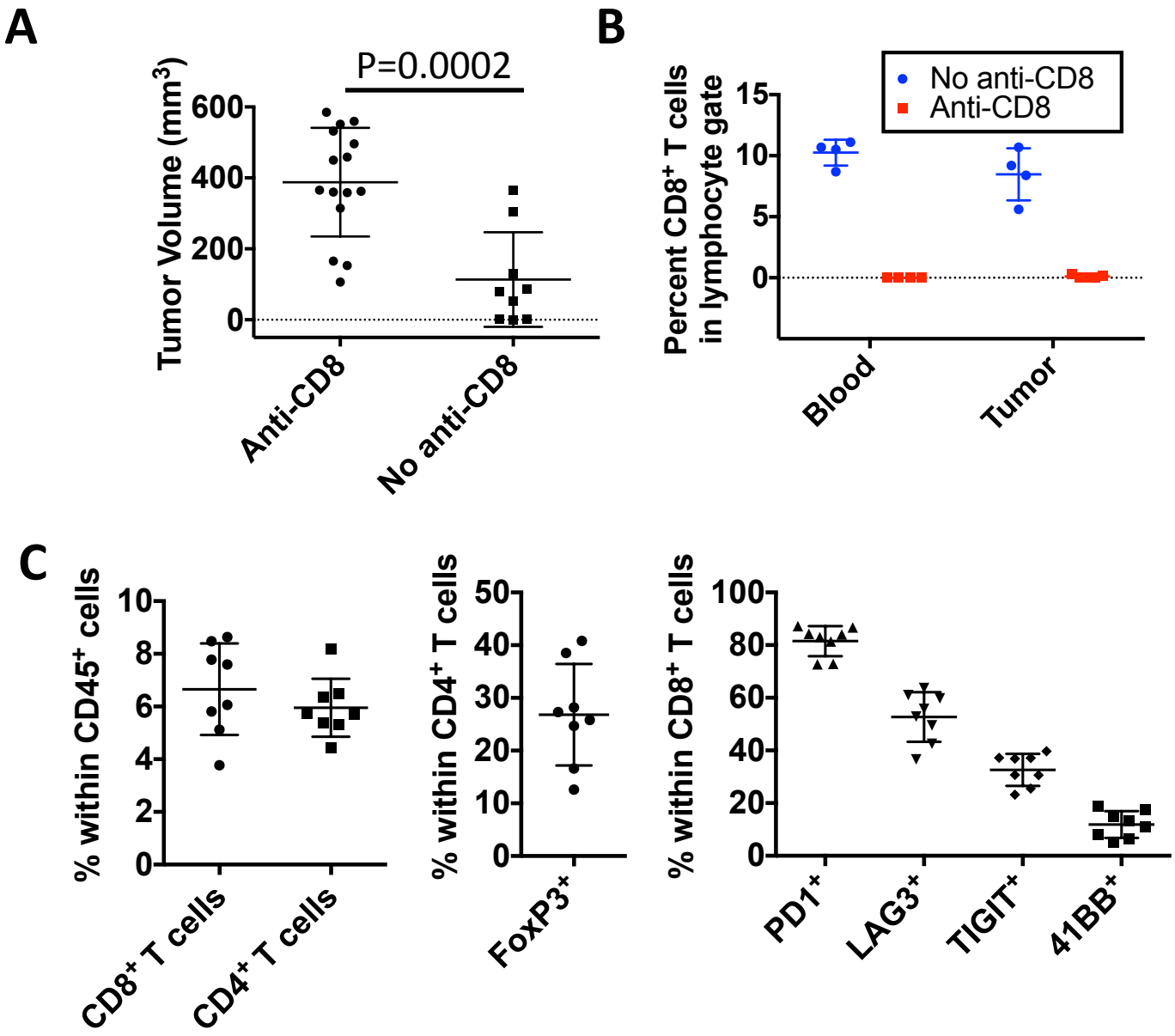

Supplementary Fig. 1. A single dose of depleting anti-CD8 antibodies at the time of tumor injection promotes Panc02SIYCerulean tumor growth but allows the development of an intratumoral T cell infiltrate with an exhausted phenotype by the time of treatment with IR. A. B6 mice were injected with $5x10^6$ Panc02SIYCerulean. Mice received or not a single 200 µg dose of anti-CD8 depleting antibodies (10F.9G2, BioXCell) on the day of tumor inoculation. Shown tumor size at day 27-29 since tumor cell inoculation (unpaired t-test). Data were pooled from 4 individual experiments. **B.** Anti-CD8 antibody depletes tumor-infiltrating T cells in addition to circulating T cells. Levels of $CD8^+$ T cells in the blood and tumors of mice bearing established MC38 tumors and treated 24 h before sacrifice with a single 200 ug dose of anti-CD8 antibodies. Control mice were untreated. 4 mice per condition. **C.** Characterization of the Panc02SIYCerulean intratumoral T cell phenotype at the time mice are treated with IR (3 weeks). Mice were injected with $5x10^6$ Panc02SIYCerulean and a single 200 µg dose of anti-CD8 at day 0. Each dot is an individual mouse. Data are from one experiment with 8 mice. All plots show average and S.D.

Supplementary Fig. 2

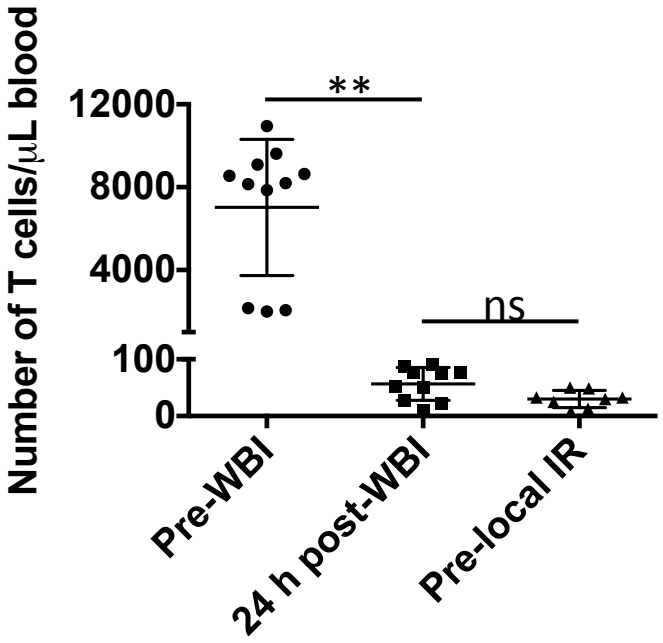

Supplementary Fig. 2. Circulating EYFP$^+$ T cells are significantly decreased after 8 Gy WBI and remain at low levels at the time of treatment with local IR . Panc02SIYCerulean cancer cells were injected s.c. into T cell reporter mice. On day 21, mice received 8 Gy WBI while tumors were shielded as in Figure 1. The number of EYFP$^+$ cells was measured in the peripheral blood before WBI, 24 h after WBI, and immediately before tumor treatment with local IR (day 5 after WBI). N=8-11 mice, shown average and S.D. **, P=002; ns, non-significant, Wilcoxon test) . An experiment is shown from 2 independent experiments with similar results.

Supplementary Fig. 3

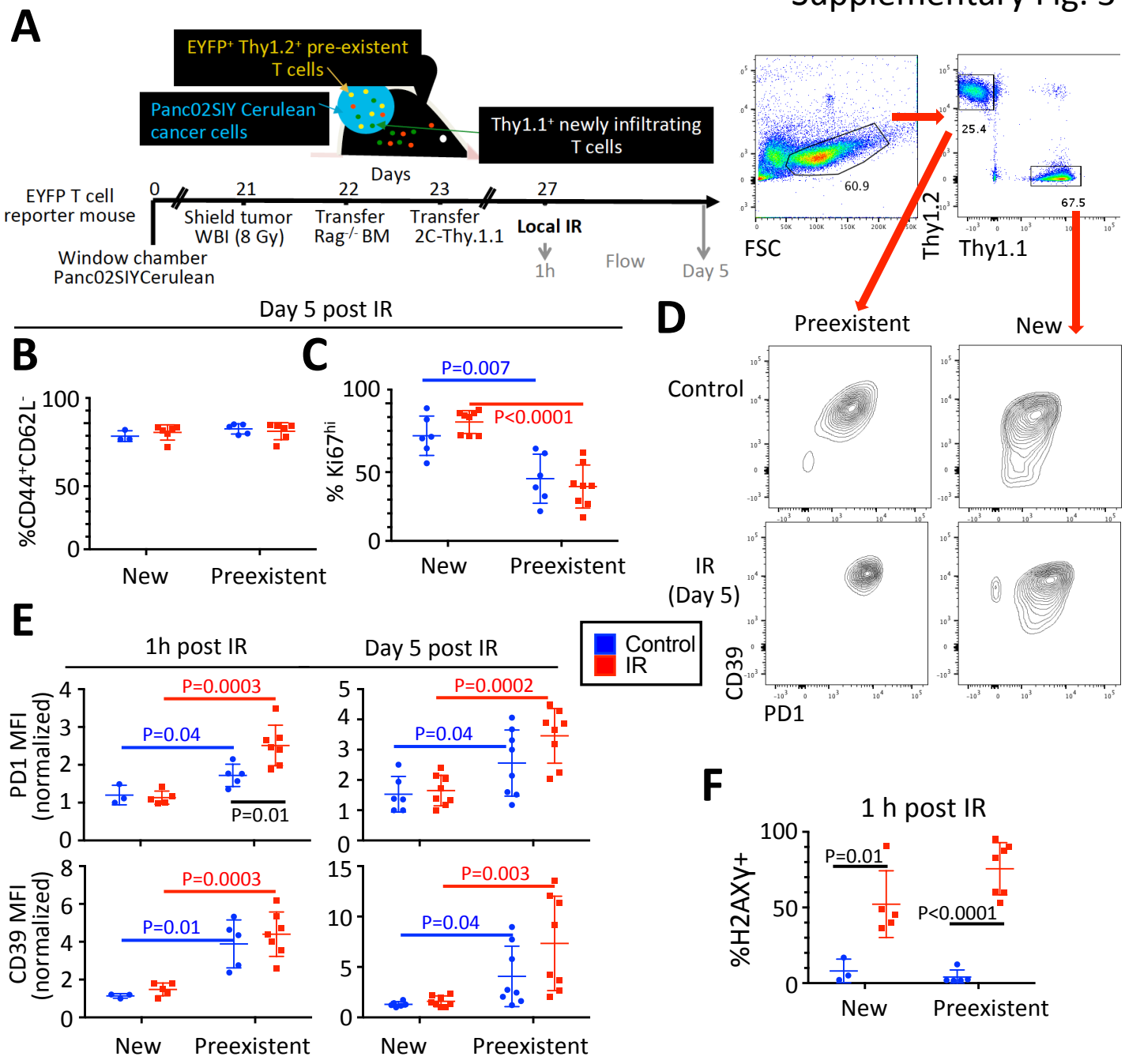

Supplementary Fig. 3. Phenotypes of preexistent and newly infiltrating T cells in tumors treated or not with IR. A. Experimental scheme and gating strategy for preexistent and newly infiltrating T cells. Experimental design is the same as used in Figure 1, but here 2C-Thy1.1⁺ were used as "newly infiltrating" T cells instead of 2C-EGFP⁺ T cells. Mice were sacrificed 1 h or 5 days after local IR and the tumors analyzed by flow cytometry. Gating strategy on magnetically enriched CD8⁺ T cells purified from tumors. **B**. The majority of both preexistent and newly infiltrating T cells are $CD44^{+}CD62L^{-}$ **C.** Preexistent T cells express lower levels of ki67 antigen compared to newly infiltrating T cells. **D-E.** Preexistent T cells express higher levels of exhaustion-associated markers PD1 and CD39 than newly infiltrating T cells (**D**, representative examples; **E**, quantification) **F.** 1 h after local IR, T cells in irradiated tumors show evidence of DNA damage, as increased percentages of phosphorylated H2AXγ. Data are pooled from 2 independent experiments for 1 h after IR and another 2 independent experiments for Day 5, with a total N=5-7 (1h) and N=6-8 (Day 5) per group. Data in E were normalized to the minimum expression value within each experiment before pooling the data. Plots in B, C, E and F show average and S.D. and were analyzed using unpaired t-tests.

Supplementary Fig. 4

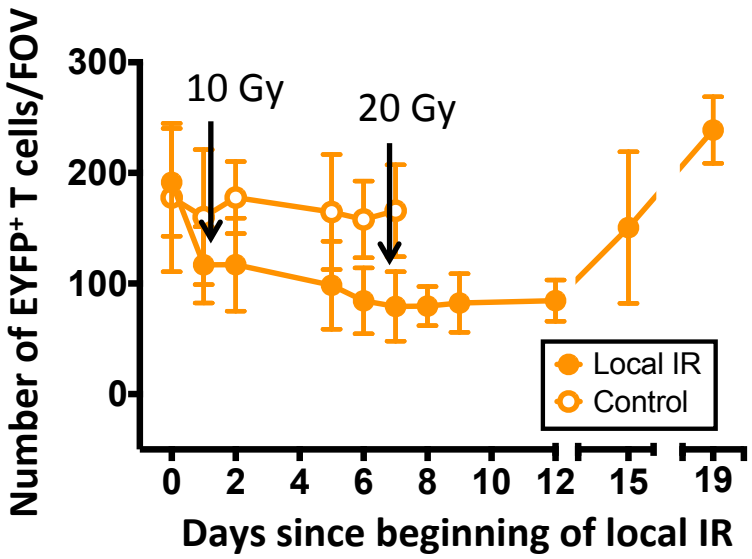

Sup. Figure 4. Survival of preexistent intratumoral T cells in MC38 tumors after 30 Gy local IR. MC38Cerulean cancer cells were injected s.c. into two T cell reporter mice (Lck-EYFP) bearing dorsal window chambers. When tumors were established (day 14), mice received a myeloablative dose (8 Gy) of WBI while their tumors were shielded, and bone-marrow was reconstituted by injection of $DsRed^{+}Rag^{-/-}$ cells within 24 h. 5 days after BM cell transfer, one mouse received 10 Gy followed by 20 Gy 4 days later as indicated in the figure. The control mouse received no local IR. Longitudinal in vivo imaging was performed on the mice before, during and after IR. Numbers of $EYFP^{+}$ T cells were determined over time in 9-13 optical regions per mouse (averages and S.D. shown).

Supplementary Fig. 5

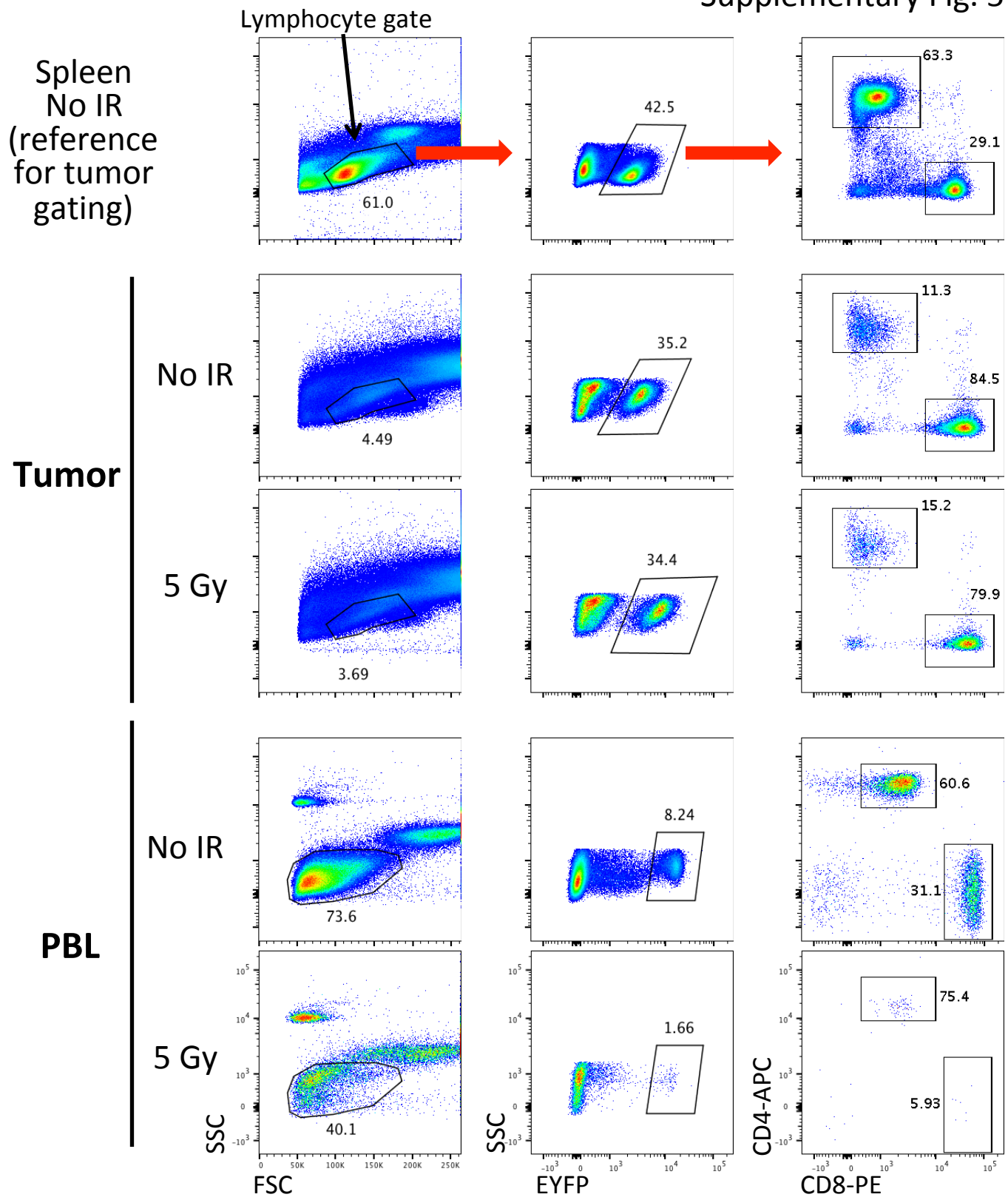

Supplementary Fig. 5. Gating strategy for determination of percentages of circulating and intratumoral T cells in T cell reporter mice receiving WBI (related to Figures 3A and 3B). Gates were first drawn on a spleen sample stained in parallel (top) and then copied into tumor sample plots. Gates for PBL samples were drawn independently since samples were processed in a different fashion as detailed in Materials and Methods. The % EYFP$^+$ (T) cells were determined in the lymphocyte gates as drawn above. Then the distribution of EYFP$^+$ T cells in CD4$^+$ and CD8+ T cells was analyzed as indicated.

Supplementary Fig. 6

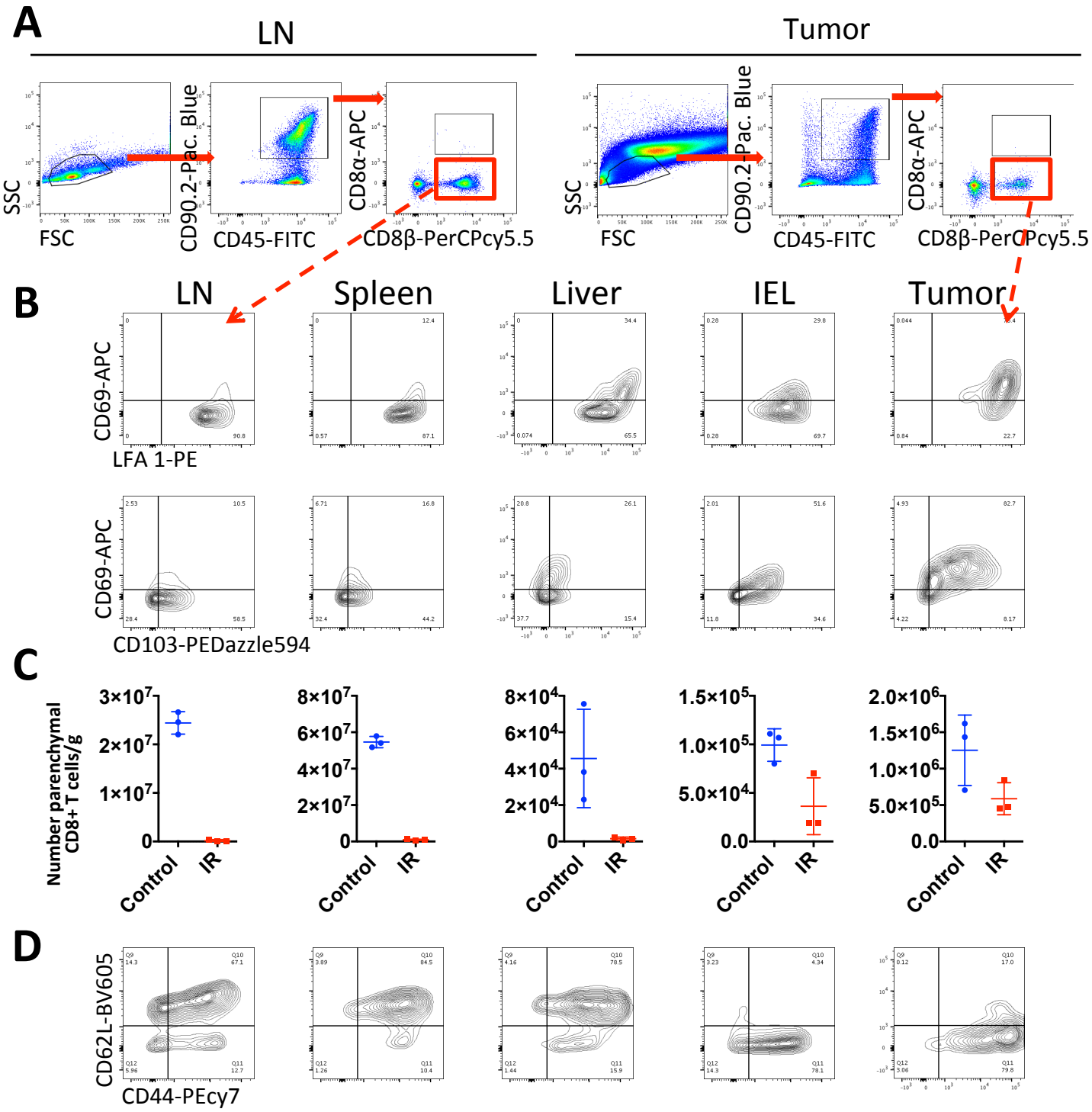

Supplementary Fig. 6 (related to Figure 3). Phenotype of parenchymal CD8⁺ T cells in MC38 tumor-bearing mice. B6 mice bearing established MC38 tumors were injected with anti-CD8α-APC i.v. Five minutes later, they were sacrificed and perfused with PBS, and their organs were extracted. **A.** Gating strategy for parenchymal CD8⁺ T cells is shown in representative examples of LN and tumor; the same strategy was used for all tissues/organs. **B.** Flow cytometry plots showing expression of markers associated with a T_{RM} phenotype by parenchymal CD8⁺ T cells from different organs/tissues. **C.** Absolute numbers of parenchymal CD8⁺ T cells in several organs before/after 8 Gy WBI (average and S.D.). **D.** Expression of markers associated with a memory phenotype by parenchymal CD8⁺ T cells. Data are from one experiment with 3 mice per group, representative of two experiments performed with similar results. Samples used for this figure are the same as used in main Fig. 3C-F.

Supplementary Fig. 7

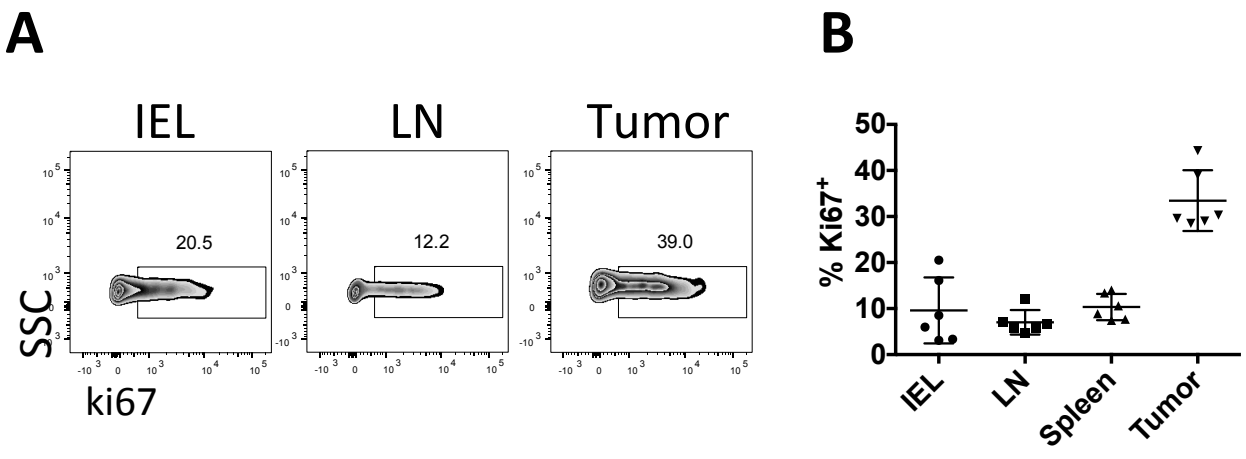

Supplementary Fig. 7. **Ki67 expression levels in radiosensitive and radio-resistant T cells.** Single cell suspensions from the indicated organs were analyzed by flow cytometry to determine the % of $Ki67^+$ cells in the $CD90.2^+CD8\beta PerCPcy5.5^+CD8\alpha APC^-$ (parenchymal $CD8^+$ T cell) population. N=6 mice. A. Representative examples for IEL, LN and tumor, B. Data summary, showing average and S.D.

Supplementary Fig. 8

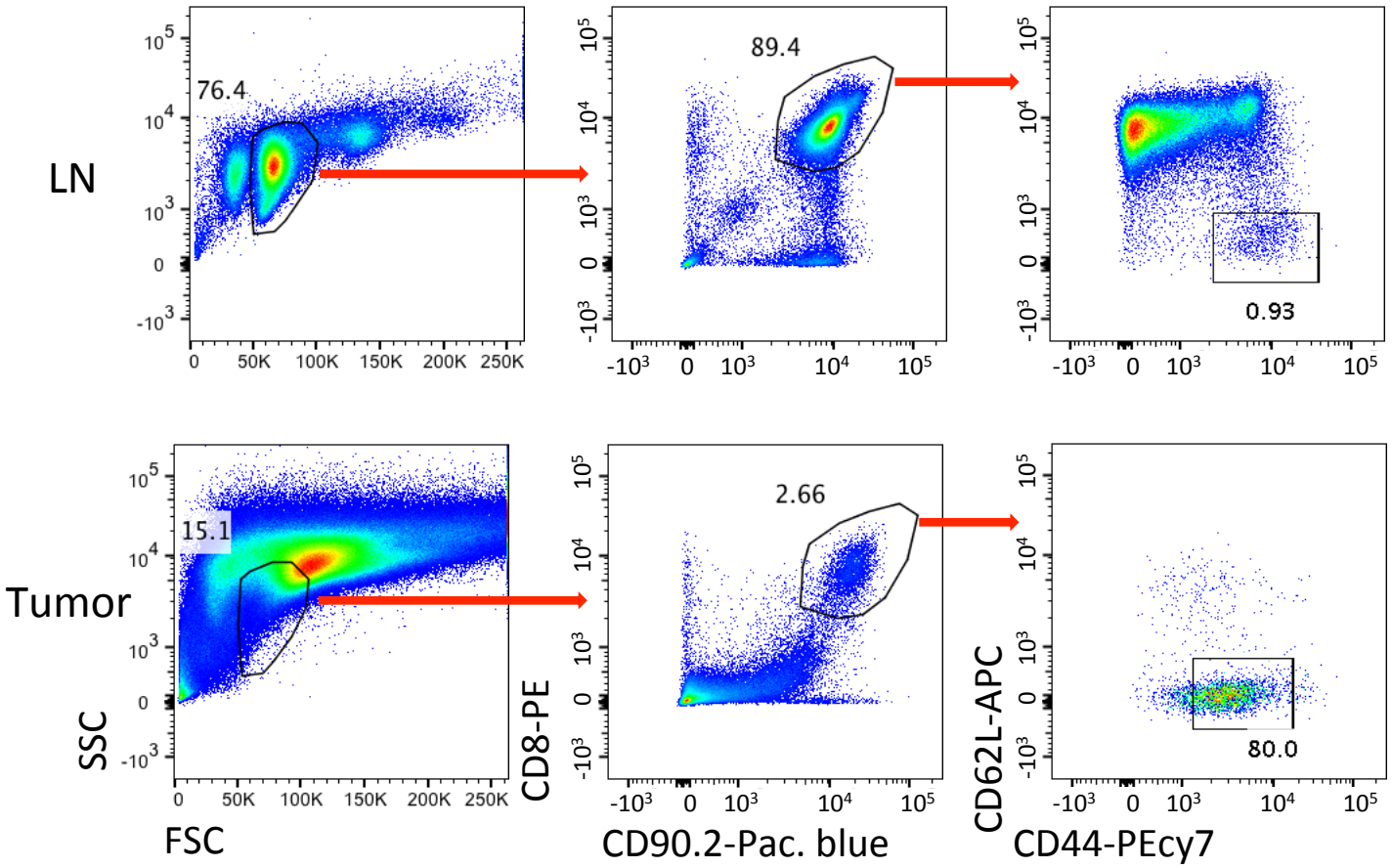

Supplementary Fig. 8 (related to Fig. 4). Sorting gates used for isolation of CD44^{+}CD62L^{-} CD8^{+} T cells from lymph nodes and tumor of MC38 tumor-bearing mice. A representative example is shown from non-irradiated mice in one out of 2 independent experiments.

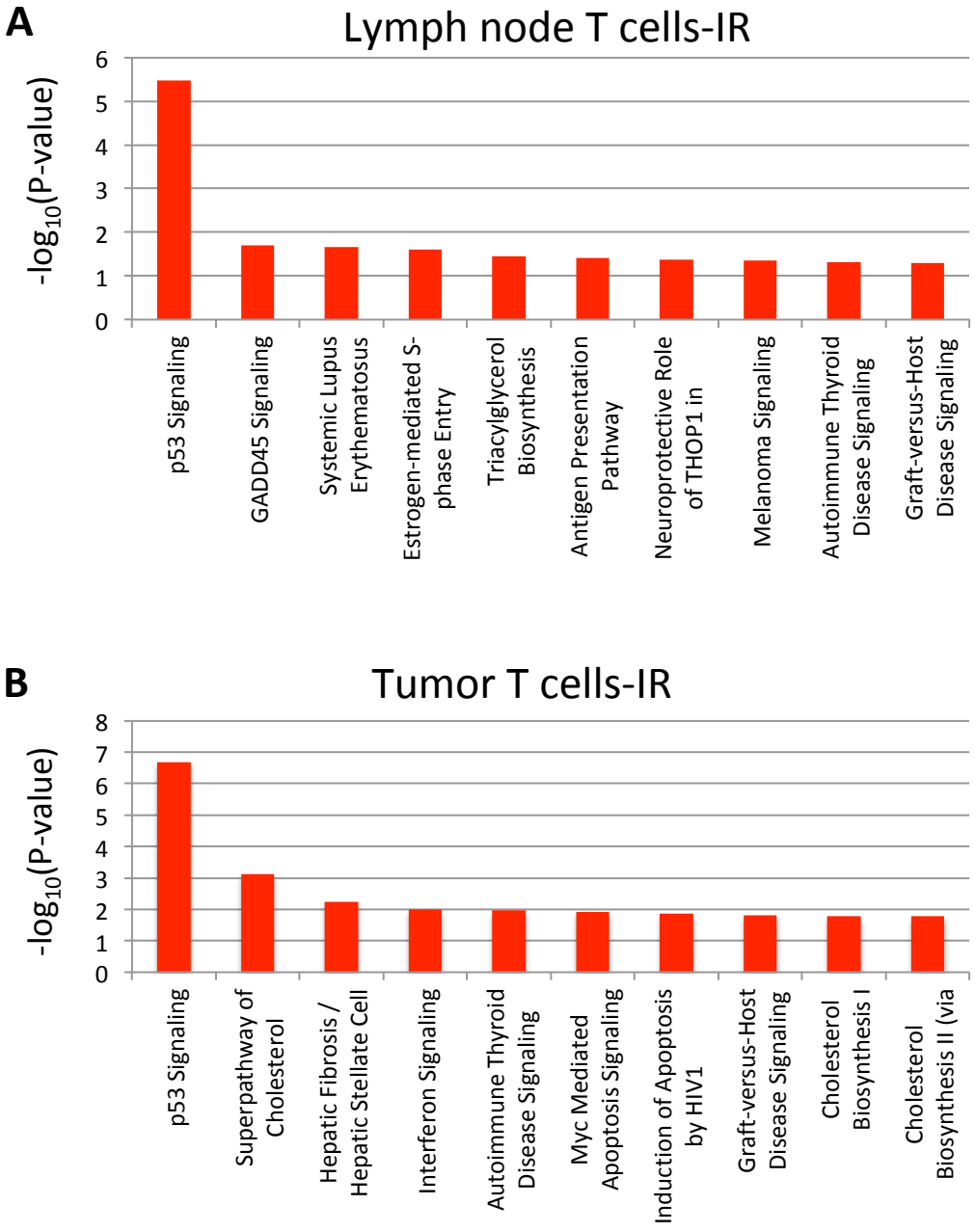

Supplementary Fig. 9. IR induces predominantly p53-signaling-related changes both in LN and tumor-infiltrating CD44^{+}CD62L^{-} T cells. Top-ranked canonical pathways activated by IR in LN- and tumor-infiltrating CD44+CD62L- T cells, respectively, as determined by IPA analysis. P-value indicates enrichment for specific canonical pathway.

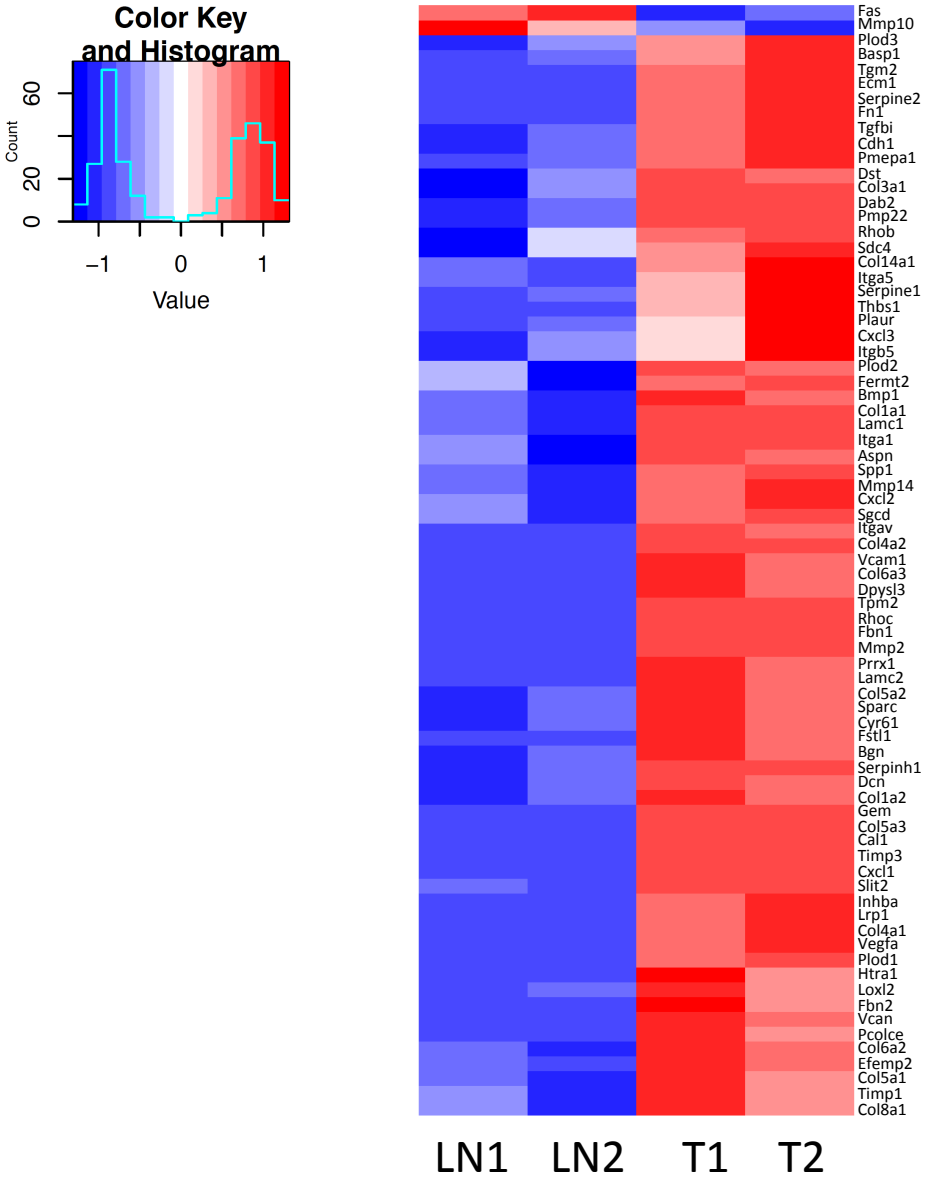

Supplementary Fig. 10. Genes from epithelial to mesenchymal transition hallmark signature (GSEA) that are differentially expressed in tumor vs. lymph node T cells. Heat map. Each array sample corresponds to pooled sorted $CD8^{+}CD44^{+}CD62L^{-}$ cells from inguinal and axillary LN (LN) or tumors (T) from 4 mice, in two independent experiments, generating 4 samples (LN1, LN2, T1, T2).

Supplementary Fig. 11

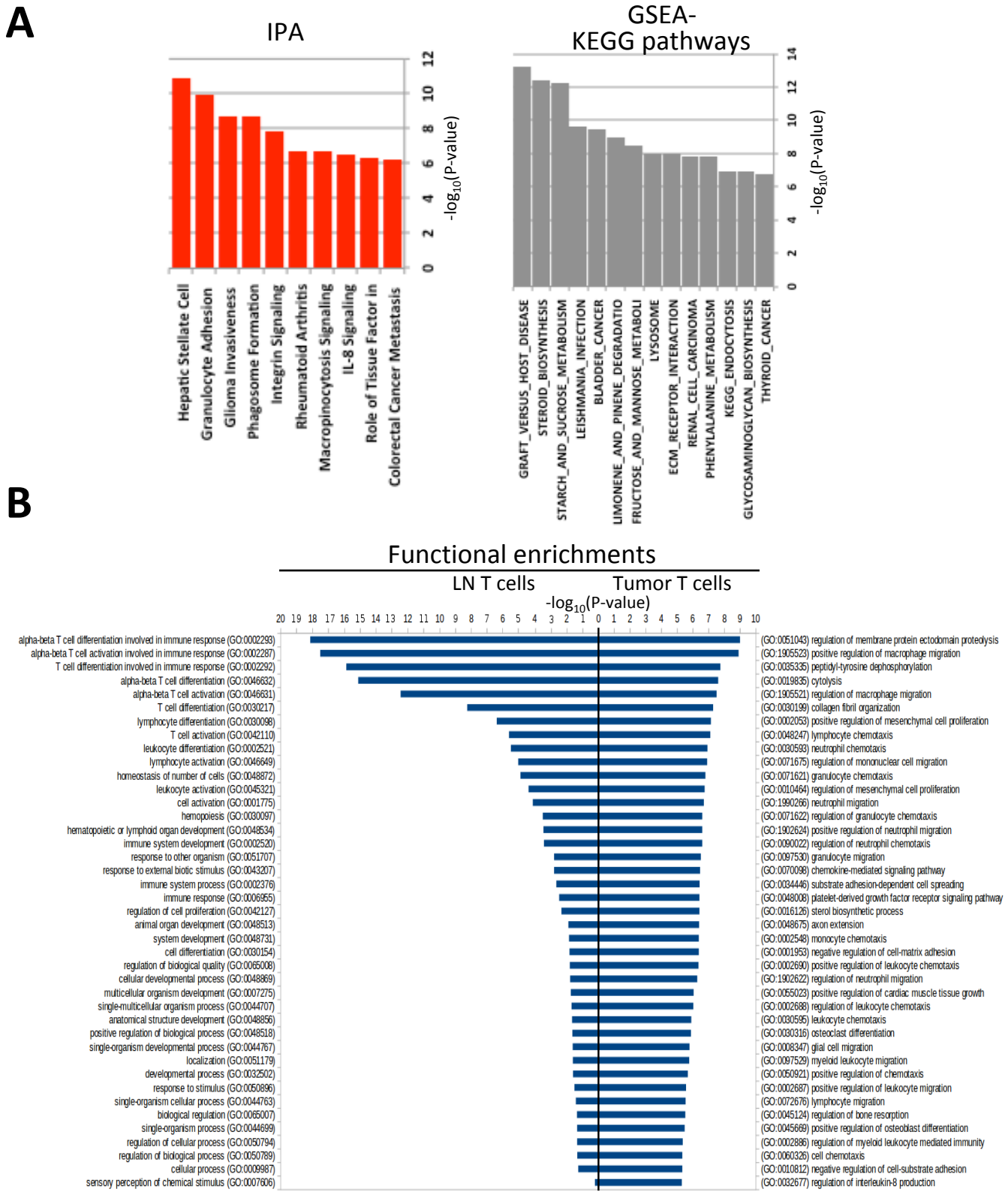

Supplementary Fig. 11. Intratumoral T cells show an activation of molecular pathways reflecting the tumor microenvironment in which they reside, and a reduction of T cell activation/differentiation-related gene expression. For Panel A, genes differentially expressed between LN and tumor T cells were analyzed using IPA (left) and GSEA (right). In Panel B, enrichment of Gene Ontology (GO) terms for genes over-expressed in LN T cells (left) and tumor T cells (right) are shown. P-value indicates enrichment for pathways or GO terms.

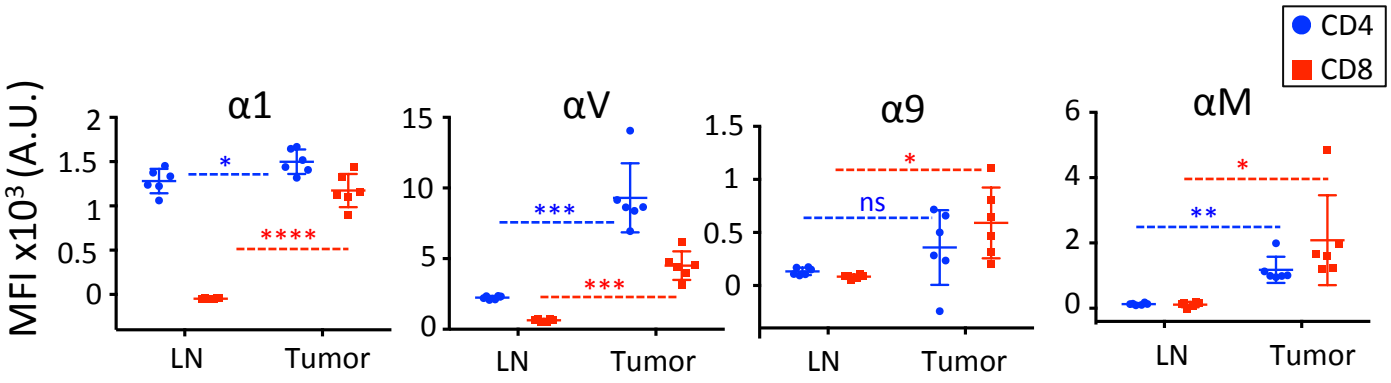

Supplementary Fig. 12. Validation of integrin subunit upregulation in intratumoral T cells at the protein level. Flow cytometry analysis of integrin expression by T cells in the tumor and LN from mice with established MC38 tumors (N=6 mice). Data are representative from 3 independent experiments and show average and S.D. *, P ≤ 0.05; ** P ≤ 0.01; ***, P ≤ 0.001; ****, P ≤ 0.0001, ns, non-significant (unpaired t-test).

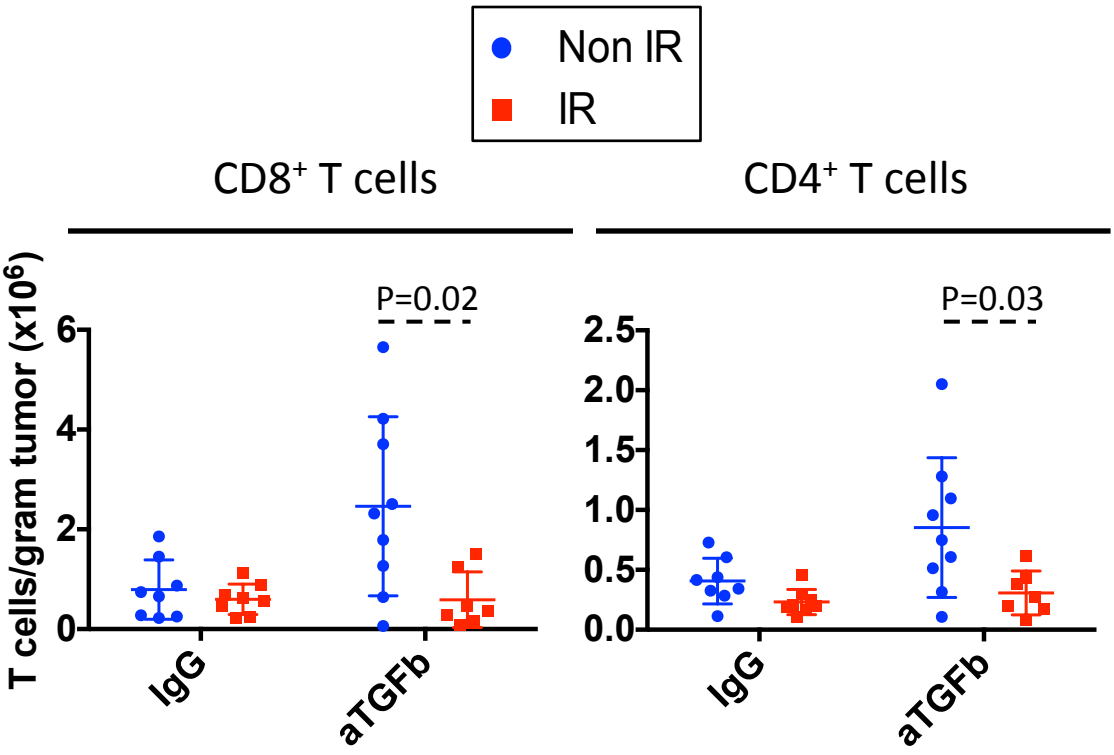

Supplementary Fig. 13. The increased effect of IR in the number of intratumoral T cells after TGFβ blockade affects CD4⁺ and CD8⁺ T cells similarly . Distribution of CD8⁺ and CD4⁺ T cells in the tumors of irradiated mice treated with TGFβ-blocking antibodies (aTGFb) or isotype control antibodies (IgG). Data correspond to the experiments shown in Fig. 5C and show average and S.D. , P values by unpaired t-test.

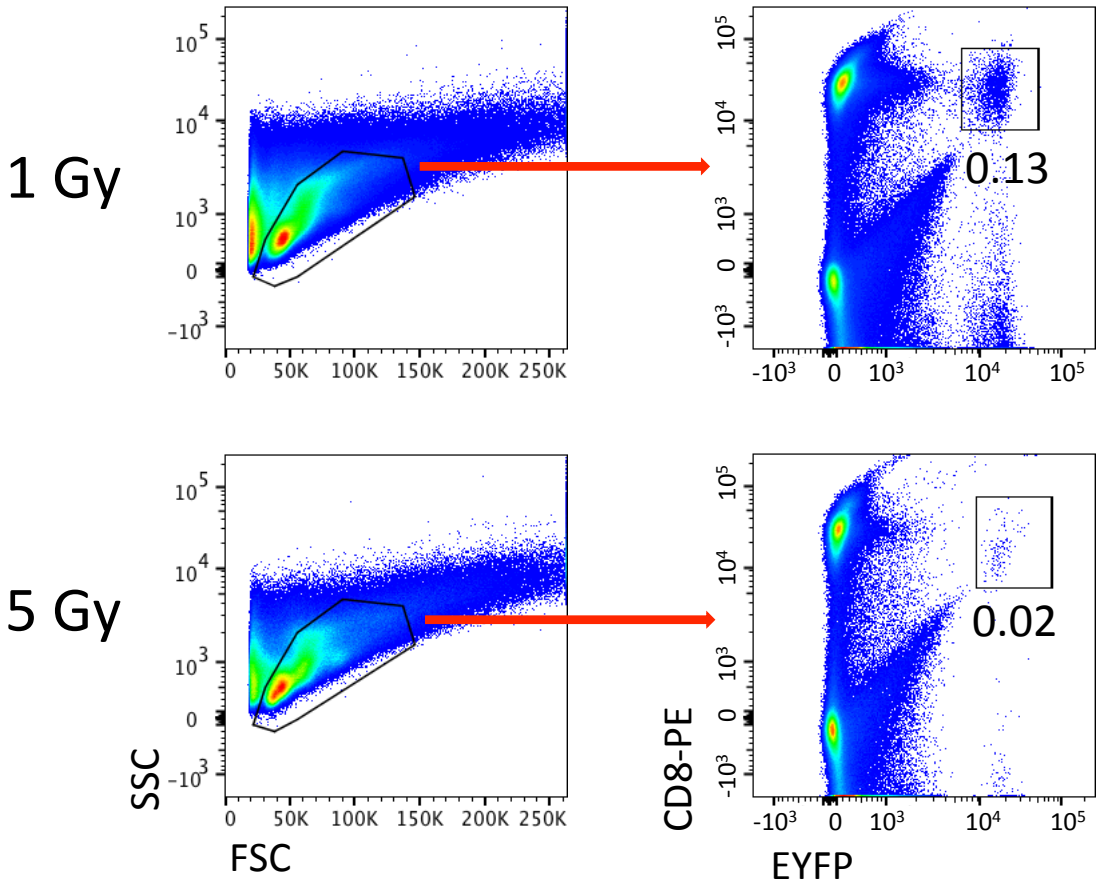

Supplementary Fig. 14 (related to Fig. 6A). Gating strategy used to quantify the levels of CD8$^+$EYFP$^+$ T cells present in recipient mice of tumor fragments from mice treated with different doses of WBI. Representative examples show splenocytes from OT1Rag$^{-/-}$ mice that were inoculated with MC38 tumor fragments grown in EYFP$^+$ T cell reporter mice treated with the indicated doses of WBI. OT1Rag$^{-/-}$ mice were sacrificed 3 weeks after tumor fragment inoculation.

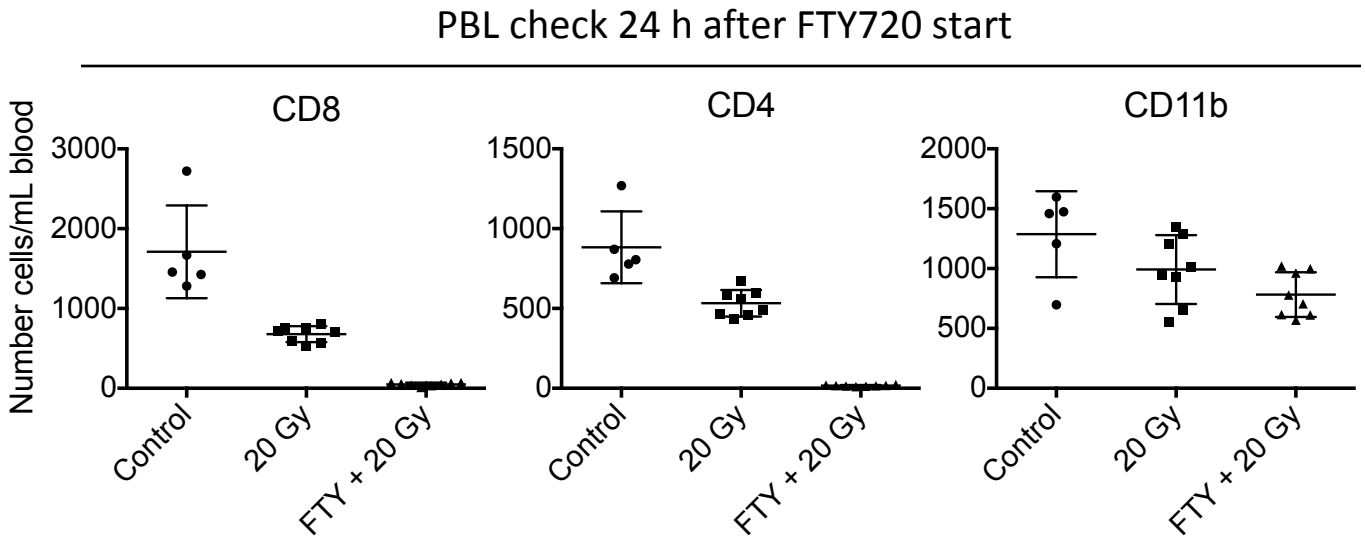

Supplementary Fig. 15. FTY720 treatment effectively eliminates circulating T cells. Absolute numbers of circulating $CD8^+$/$CD4^+$ T cells and $CD11b^+$ cells (control) were determined in mice treated or not with FTY720 in Figure 6C to verify its activity. Shown average and S.D.

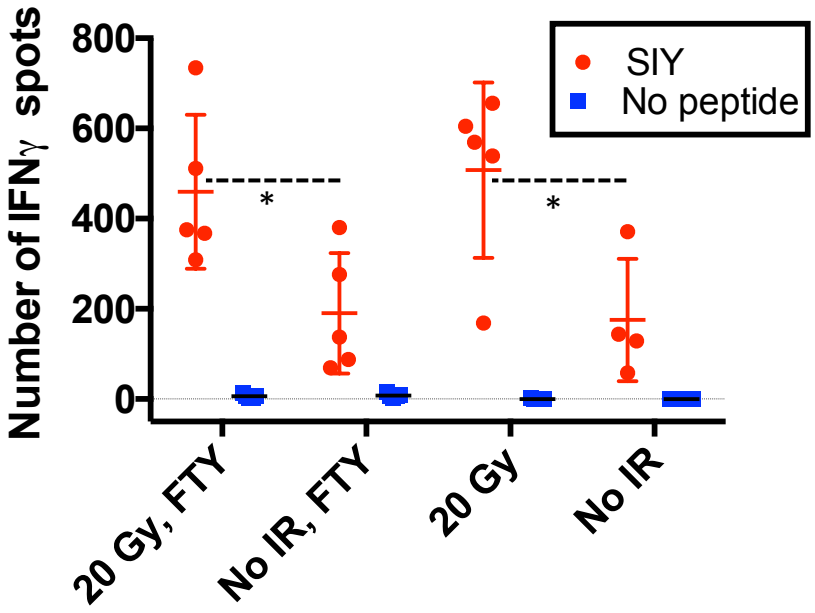

Supplementary Fig. 16. IFNγ production by T cells from irradiated tumors in mice treated or not with FTY720. T cells were purified from irradiated Panc02SIYCerulean tumors 9 days after 20 Gy local IR, and their IFNγ production was analyzed by ELISPOT. Mice were treated or not with FTY720 every 24 h starting 24 h before IR to prevent new T-cell infiltration. Data are from one experiment out of two performed with similar results. Each dot is an individual mouse; shown average and S.D. *, P<0.05. **, P<0.01 (unpaired t-test).

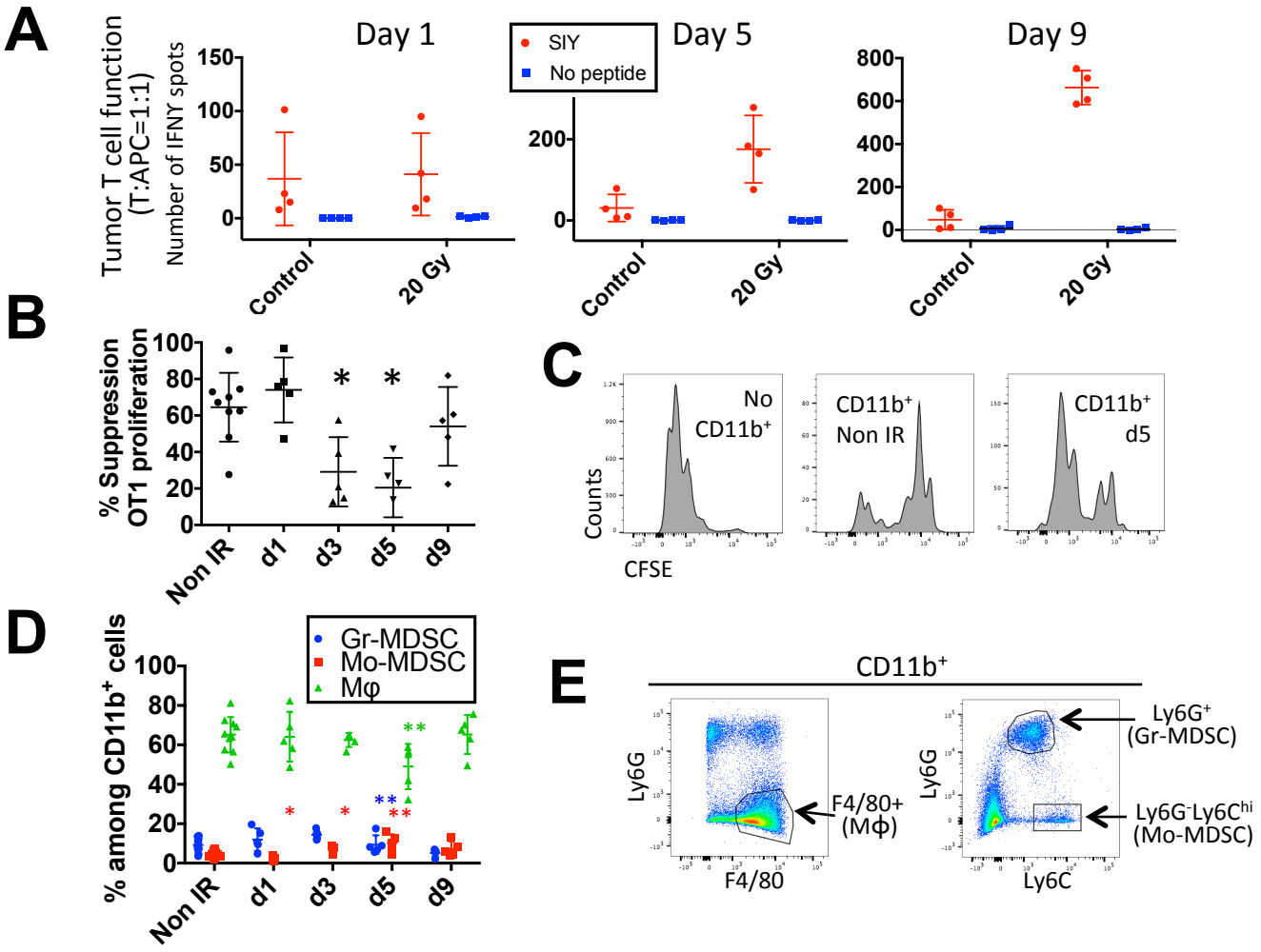

Supplementary Fig. 17. Changes in T cell and myeloid cell function and phenotype in tumors from mice receiving high dose local IR and FTY720 (related to Fig. 6C). Established (3 week) Panc02SIYCerulean tumor-bearing mice were treated or not with 20 Gy local IR. All mice received FTY720 via oral gavage every 24 h starting 24 h before IR until completion of the experiment to prevent new T cell infiltration. **A.** Production of IFNγ by T cells purified from irradiated tumors at days 1, 5 and 9 after IR, measured by ELISPOT. Each dot is an individual mouse. **B.** $CD11b^+$ cells were purified from tumors treated as in A, and incubated with CFSE-labeled OT1 splenocytes and OVA peptide to test their ability to suppress T cell proliferation at different times after IR. N=5 mice per group except Non IR (N=9). **C.** Representative FACS plots showing CFSE dilution by OT1 cells in control wells (no $CD11b^+$ added) or wells with $CD11b^+$ cells purified from untreated mice (Non IR) or mice treated with 20 Gy , at day 5 after IR (d5). **D.** Distribution of $CD11b^+$ cells from B in myeloid cell subsets. **E.** Gating strategy used for D. B-E: Two experiments were performed, one comparing tumors that had been irradiated 1 or 3 days before the experiment, vs. non-irradiated tumors; in a second experiment, mice received IR 5 or 9 days before sacrifice, or were not irradiated. In B and D, control unirradiated mice from the two experiments were pooled ("Non IR") and each subset and time point was compared to pooled Non IR. Shown average and S.D; P values by unpaired t-test. *, $P<0.05$. **, $P<0.01$.

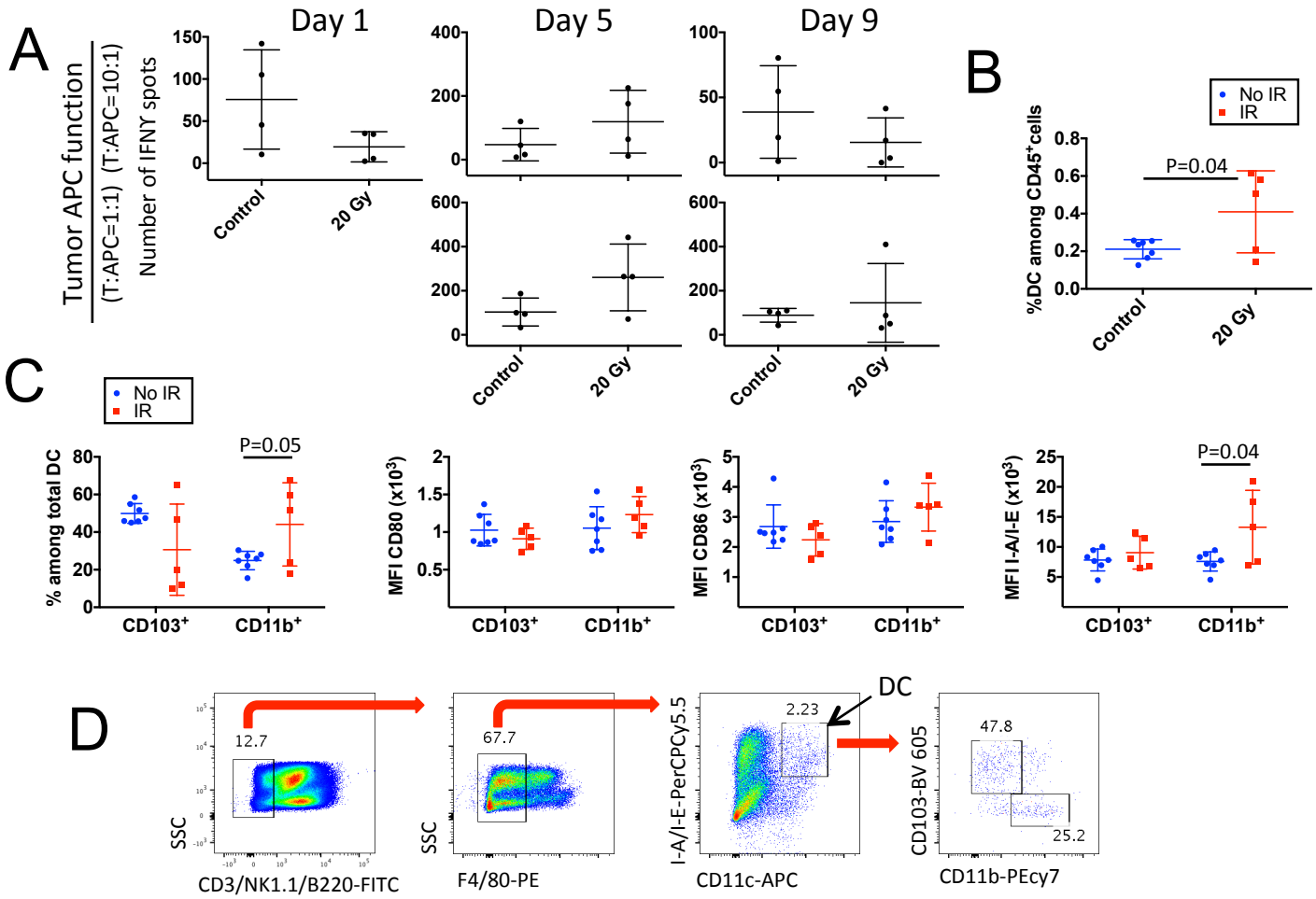

Supplementary Fig. 18. Changes in DC numbers and phenotype in tumors from mice receiving local high dose IR and FTY720 treatment to prevent new T cell infiltration (related to Fig 6C). A. Production of IFNγ by 2C T cells stimulated with CD11c$^+$ cells (APC) purified from the same tumors used in Suppl. Fig. 17. Each dot represents an individual mouse. **B-D.** Changes in DC representation and phenotype were analyzed in CD45$^+$ cells magnetically purified from tumors at day 5 after IR. Each dot represents an individual mouse. **B.** % CD11c$^+$MHC-II$^+$ (DC) cells in total CD45$^+$ cells, and **C.** Distribution of DC in CD103$^+$/CD11b$^+$ subsets and levels of expression of DC activation markers on each subset in unirradiated vs. irradiated tumors. **D.** Gating strategy used to defineCD103$^+$ and CD11b$^+$ DC subsets. Shown average and S.D; P values by unpaired t-test.

Supplementary Fig. 19

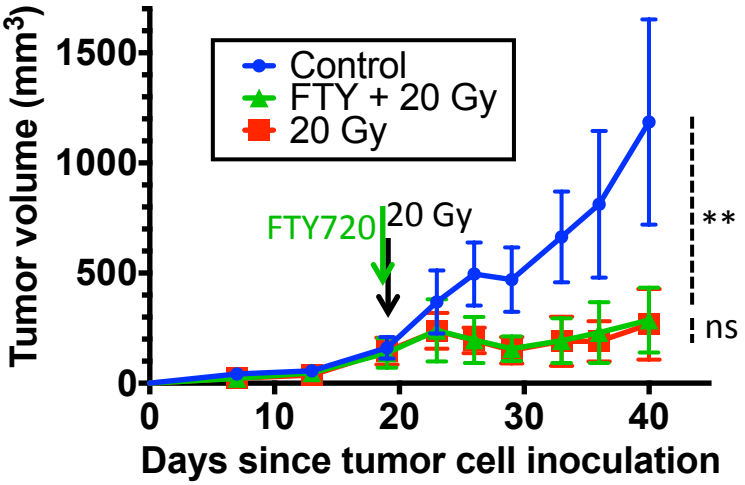

Supplementary Fig. 19. Intratumoral preexistent T cells suffice to control Panc02SIYCerulean tumors without the contribution of newly infiltrating T cells. B6 mice bearing Panc02SIYCerulean s.c. tumors were treated at day 19 after tumor-cell inoculation with 20 Gy local IR. Some mice also received 20 µg FTY720 (FTY) via oral gavage every 24 h, starting 3 h before IR and until day 40. N=8 mice per group except control (N=5). Shown average and S.D. **, P<0.01 (unpaired t-test with Welch's correction at day 40).

Supplementary Table 1. Statistical significance of differences in the effect of IR (fold decrease) in the number of parenchymal $CD8^+$ T cells/g across different tissues.

	P value summary	Geometric mean	Confidence interval	t value	df	P value
LN vs. Spleen	ns	0.9544	0.2873 to 3.171	0.1079	4	0.9193
LN vs. Liver	***	0.07793	0.03531 to 0.1720	8.286	5	0.0004
LN vs. IEL	**	0.02870	0.004797 to 0.1717	5.102	5	0.004
LN vs. Tumor	***	0.01498	0.003485 to 0.06440	7.405	5	0.0007
Spleen vs. Liver	***	0.08383	0.04636 to 0.1516	11.62	4	0.0003
Spleen vs. IEL	*	0.04232	0.005036 to 0.3557	4.125	4	0.0146
Spleen vs. Tumor	***	0.02192	0.006777 to 0.07087	2.405	4	0.0008
Liver vs. IEL	ns	0.3683	0.06025 to 2.251	1.419	5	0.2152
Liver vs. Tumor	*	0.1922	0.04673 to 0.7906	2.998	5	0.0302
IEL vs. Tumor	ns	0.5220	0.1374 to 1.983	1.252	5	0.2660

df, degrees of freedom; ns, not significant. Related to Figure 3C.

Supplementary Table 2. **GSEA Hallmark signatures enriched in tumor vs. LN T cells.**

Name	Enrichment Score	FDR q-val
Hallmark_angiogenesis	0.8134586	0
Hallmark_epithelial_mesenchymal_transition	0.7779522	0
Hallmark_cholesterol_homeostasis	0.76271915	0
Hallmark_hypoxia	0.71806777	0
Hallmark_tnfa_signaling_via_nfkb	0.70413136	0
Hallmark_coagulation	0.6979829	0
Hallmark_protein_secretion	0.6804933	0
Hallmark_uv_response_dn	0.67722726	0
Hallmark_complement	0.6621574	0
Hallmark_il6_jak_stat3_signaling	0.6590407	0
Hallmark_apoptosis	0.6571919	0
Hallmark_tgf_beta_signaling	0.6507696	4.88E-04
Hallmark_inflammatory_response	0.6401307	0
Hallmark_kras_signaling_up	0.63761026	0
Hallmark_glycolysis	0.60729474	0
Hallmark_p53_pathway	0.6036037	0
Hallmark_mtorc1_signaling	0.58386016	0
Hallmark_reactive_oxigen_species_pathway	0.5772216	0.0080058
Hallmark_adipogenesis	0.5755323	6.10E-05
Hallmark_estrogen_response_late	0.55888486	2.73E-04
Hallmark_il2_stat5_signaling	0.55768514	3.01E-04
Hallmark_myogenesis	0.55357033	2.88E-04
Hallmark_apical_surface	0.55173165	0.0150894
Hallmark_androgen_response	0.5408939	0.0036154
Hallmark_estrogen_response_early	0.5343756	0.0010496
Hallmark_apical_junction	0.53242785	6.82E-04
Hallmark_peroxisome	0.5232168	0.0047586
Hallmark_allograft_rejection	0.5225824	0.0014078
Hallmark_notch_signaling	0.5181071	0.0783368
Hallmark_hedgehog_signaling	0.5054939	0.0876418
Hallmark_interferon_gamma_response	0.49924973	0.0034960
Hallmark_mitotic_spindle	0.48338783	0.0057354
Hallmark_pancreas_beta_cells	0.47784835	0.1291808
Hallmark_heme_metabolism	0.43603775	0.0294758
Hallmark_unfolded_protein_response	0.41791424	0.0860558
Hallmark_uv_response_up	0.41009387	0.0774233
Hallmark_xenobiotic_metabolism	0.4094393	0.0601320
Hallmark_bile_acid_metabolism	0.37937248	0.2024376
Hallmark_interferon_alpha_response	0.32377967	0.5406943
Hallmark_pi3k_akt_mtor_signaling	0.31798315	0.5168584

Shown 40 top Hallmark signatures. Related to Figure 4.